UCRL-53605
Distribution Category UC-21

UCRL--53605

DE85 007494

Response of Variable Impedance Stripline to Pulse Excitation

G. McWright

Manuscript date: December 15, 1984

LAWRENCE LIVERMORE NATIONAL LABORATORY
University of California • Livermore, California • 94550

MASTER

Available from: National Technical Information Service • U.S. Department of Commerce
5285 Port Royal Road • Springfield, VA 22161 • $7.00 per copy • (Microfiche $4.50)

Contents

Response of Variable Impedance Stripline to Pulse Excitation

Abstract

We describe a simple method to predict the transient response of variable impedance stripline to pulse excitation. The method uses a finite difference based, quasi-static impedance formulation to calculate the reflection coefficient at each point along the direction of pulse propagation and the subsequent short pulse behavior of a variable impedance structure. A Fortran computer program is written to determine the quasi-static impedance. Excellent agreement of better than 1% between the finite difference impedance predictions and experimental results is noted. A second computer program is written utilizing previous results but essentially incorporating reflection and transmission from several discontinuities to analyze the transient response of the structure. This transient analysis yields good agreement between predictions and results obtained by means of time domain reflectometry.

1. Introduction

The proposed scheme for Nova temporal pulse shaping[1] utilizes passive reflection of a high voltage pulse from nonuniform stripline. The distorted voltage pulse is subsequently applied to a Pockels cell gate to realize a shaped optical pulse. Of considerable interest, then, is the transient response of variable impedance stripline to pulse excitation. In this report, we describe a simple method to predict the resultant voltage shape.

The method uses a finite difference based, quasi-static impedance formulation; the predicted quasi-static impedance is used to calculate the reflection coefficient at each point along the transmission line and the subsequent short pulse behavior of a variable impedance structure.

We review the transmission line equations in Sec. 2; calculate the quasi-static impedance and compare the finite difference calculations with experimental results in Sec. 3; analyze the transient response of the variable impedance stripline and compare predictions to measurements on the structure made with time domain reflectometry (TDR) in Sec. 4.

2. Transmission Line Fundamentals

The voltage, V, and the current, I, along a lossless, uniform transmission line (Fig. 1) are given by the telegrapher's equations[2]

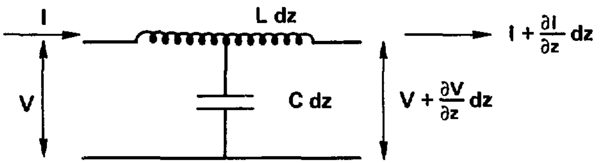

Figure 1. Equivalent circuit of transmission line.

$$\frac{\partial V}{\partial z} = -L\frac{\partial I}{\partial t} \,, \tag{1}$$

$$\frac{\partial I}{\partial z} = -C\frac{\partial V}{\partial t} \,, \tag{2}$$

where ∂z is a differential length of line, and L and C are the inductance and capacitance per unit length, respectively. Differentiating Eq. *(1) with respect to distance and* Eq. *(2) with respect to time, we obtain*

$$\frac{\partial V^2}{\partial z^2} = LC\frac{\partial V^2}{\partial t^2} \,. \tag{3}$$

Similarly,

$$\frac{\partial I^2}{\partial z^2} = LC\frac{\partial I^2}{\partial t^2} \,. \tag{4}$$

The solution of Eq. (3) is

$$V = F_1(t - z/v) + F_2(t + z/v) \,, \tag{5}$$

where F_1 and F_2 are arbitrary functions of $(t - z/v)$ and $(t + z/v)$, respectively, and the phase velocity, v, is

$$v = \frac{1}{\sqrt{LC}} \,. \tag{6}$$

Substituting Eq. (5) into Eq. (1) and integrating with respect to t, we obtain

$$I = \frac{1}{Z_0}\left[F_1(t - z/v) - F_2(t + z/v)\right] \,, \tag{7}$$

where the characteristic impedance, Z_0, is

$$Z_0 = \sqrt{\frac{L}{C}} \,. \tag{8}$$

Of particular interest is the junction between a given uniform line and a line of different characteristic impedance. The total voltage in the line may be regarded as the sum of a voltage in a positive traveling wave equal to V_+ at the point of discontinuity and a voltage V_- in a reflected wave. Then

$$V_+ + V_- = V_L \,, \tag{9}$$

where V_L is the voltage appearing across the the load impedance, Z_L. Also, the sum of the currents in the positive and negative traveling waves of the line at the discontinuity must equal the current into Z_L:

$$I_+ + I_- = I_L \,. \tag{10}$$

Then

$$\frac{V_+}{Z_0} - \frac{V_-}{Z_0} = \frac{V_L}{Z_L} \,. \tag{11}$$

Most importantly, the reflection coefficient, ρ, and transmission coefficient, τ, are

$$\rho = \frac{V_-}{V_+} = \frac{Z_L - Z_0}{Z_L + Z_0} , \tag{12}$$

$$\tau = \frac{V_L}{V_+} = \frac{2Z_L}{Z_L + Z_0} . \tag{13}$$

3. Quasi-Static Impedance Formulation

In this section, we use a finite difference approach to calculate the impedance of stripline. The finite difference predictions are subsequently compared with experimental results.

3.1 Theory

A cross section of the strip transmission line of interest, here, is shown in Fig. 2. Surrounded by ground planes, the line consists of a strip to which microwave signal is applied. We are interested in determining the impedance

$$Z_0 = \sqrt{\frac{L}{C}} = \frac{\sqrt{\mu\epsilon}}{C} . \tag{14}$$

We will first calculate the potential throughout the structure using a finite difference equation for the Laplace operator.[3,4] The function $U(x,y)$ satisfies the linear second-order partial differential equation

$$U_{xx} + U_{yy} = 0 , \tag{15}$$

with the boundary conditions

$$U(x,y) = U_1 = 1 \quad \text{(boundary 1)} , \tag{16}$$

$$U(x,y) = U_0 = 0 \quad \text{(boundary 2)} . \tag{17}$$

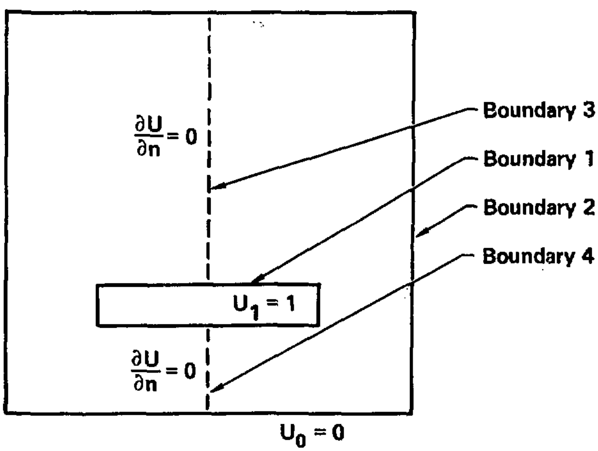

Figure 2. Cross section of strip transmission line.

Figure 3(a). Notation for Eq. (19).

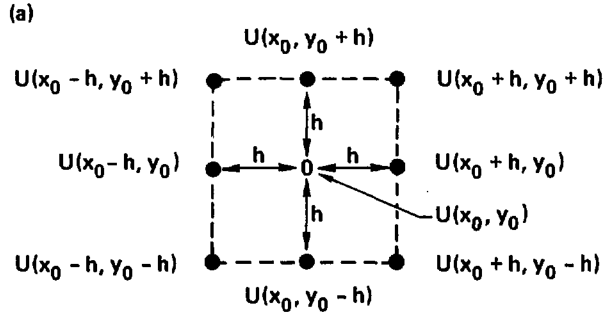

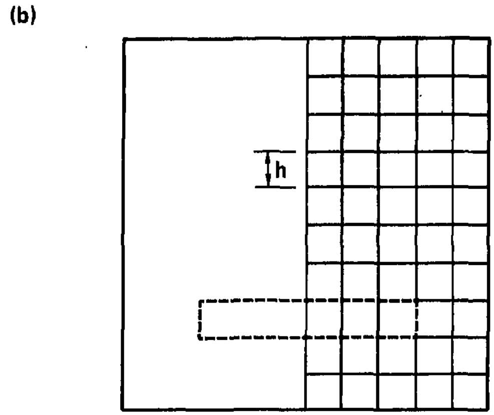

Figure 3(b). Stripline with mesh superimposed.

The problem can be simplified considerably by using the line of symmetry with the additional boundary conditions

$$\frac{\partial u}{\partial n} = 0 \quad \text{(boundaries 3 and 4)} \; . \tag{18}$$

A square mesh with an arbitrary mesh size, h, is now superimposed on the sub-domain. By using the notation of Fig. 3, assuming that $U(x,y)$ has partial derivatives of fourth order near the interior mesh point (x_0,y_0), and by using Taylor's theorem, we obtain

$$U_{xx}(x_0,y_0) = \frac{U(x_0 + h,y_0) + U(x_0 - h,y_0) - 2U(x_0,y_0)}{h^2} - \frac{h^2}{4!}\left[U_{xxxx}(\xi_1,y_0) + U_{xxxx}(\xi_2,y_0)\right] , \tag{19}$$

$$U_{yy}(x_0,y_0) = \frac{U(x_0,y_0 + \eta) + U(x_0,y_0 - \eta) - 2U(x_0,y_0)}{h^2} - \frac{h^2}{4!}\left[U_{yyyy}(x_0,\eta_1) + U_{yyyy}(x_0,\eta_2)\right] , \tag{20}$$

The coordinates ξ_1, ξ_2, η_1, and η_2 satisfy the following conditions:

$$x_0 - h < \xi_1 < x_0 < \xi_2 < x_0 + h \; , \tag{21}$$

$$y_0 - h < \eta_1 < y_0 < \eta_2 < y_0 + h \ . \qquad (22)$$

Combining (15), (19), and (20) we obtain

$$U(x_0 + h, y_0) + U(x_0 - h, y_0) + U(x_0, y_0 + h) + U(x_0, y_0 - h) - 4U(x_0, y_0) = \delta(h^4) \ , \qquad (23)$$

where $\delta(h^4)$ is an error term of fourth order.

Methods for the solution of Eq. (23) along with the associated error analysis have been reviewed extensively.[5-7] The relaxation technique consists of approximating the function $U(x,y)$ with a function $U_{j,k}$ which is only defined for each discrete mesh point. The potential values are continuously modified until all of the simultaneous equations are satisfied to a sufficient degree of accuracy. The simplest numerical procedure is the Liebmann method[4] in which the lattice is scanned along successive columns, and old values for each mesh point are discarded and replaced by new ones. The relaxation formula for the new value of $U_{j,k}^{n+1}$ is

$$U_{j,k}^{n+1} = \frac{1}{4}\left(U_{j-1,k}^{n+1} + U_{j+1,k}^{n} + U_{j,k-1}^{n+1} + U_{j,k+1}^{n}\right) , \qquad (24)$$

and the potential throughout the structure is thus calculated.

To obtain the capacitance, C, and thus the impedance, Z, it is necessary to calculate the charge Q, on the conductors.[8] If we form a Gaussian surface with lines parallel to the coordinate directions (Fig. 4), at any point P on this surface

$$D_n = \epsilon E_n = -\epsilon \frac{\partial u}{\partial n} \ , \qquad (25)$$

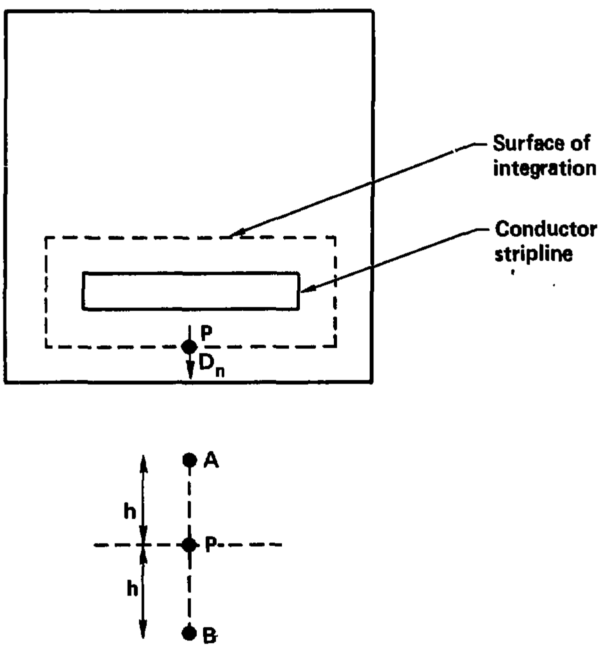

Figure 4. Stripline with Gaussian surface of integration.

where n is the normal coordinate and D_n and E_n are the normal components of the displacement and electric intensity, respectively. Expressing E_n numerically,

$$-E_n = \frac{\partial U}{\partial n} = \frac{U_B - U_A}{2h} , \tag{26}$$

where U_B and U_A are the potentials on either side of P. Thus, if the surface containing the conductor consists of S straight line segments each containing v nodes, the charge per unit length normal to the cross section is

$$Q = \epsilon h \left[\sum_{S} \sum_{P=1}' \left(\frac{\partial U}{\partial n} \right)_P \right] , \tag{27}$$

where the symbol Σ' is used to indicate that th. first and last terms in the summation are halved. Then

$$C = \frac{Q}{V} , \tag{28}$$

where V is the potential difference between the conductors (unity) and the impedance is thus determined.

3.2 Programming Details

A Fortran computer program (Appendix 1) implementing the techniques of Sec. 3.1 was developed. The program may be divided into three sections:

3.2.1 Location Loader
3.2.2 Relaxation Process
3.2.3 Capacitance Calculation

3.2.1 Location Loader

The relevant structure is shown in Fig. 5, superimposed on a matrix of size Y by Z. The location of the inner conductor, the matrix size, and the number of relaxation cycles are input by the operator in the following order:

UL1, UL2, UR1, UR2, LL1, LL2, LR1, LR2, Y, Z, N

where

UL1, UL2 are row, column of upper left coordinate of inner conductor,

UR1, UR2 are row, column of upper right coordinate of inner conductor,

LL1, LL2 are row, column of lower left coordinate of inner conductor,

LR1, LR2 are row, column of lower right coordinate of inner conductor,

Y, Z are row, column of complete structure,

N is the number of relaxation cycles.

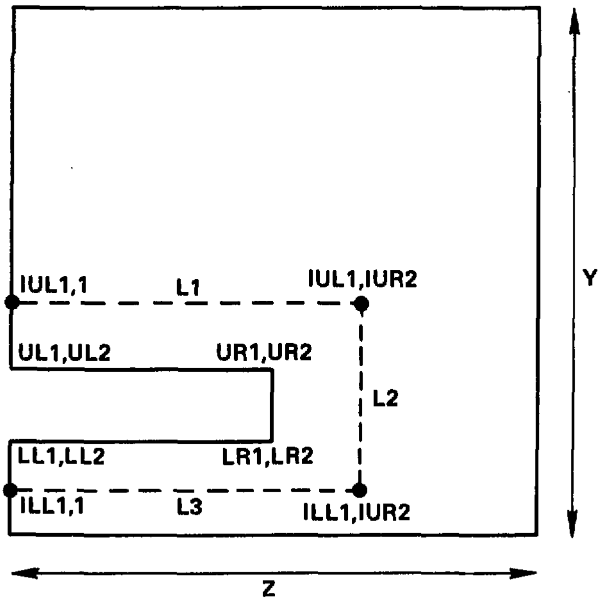

Figure 5. Line segments for capacitance calculation.

A constant potential $U_I = 1$ is assigned to all mesh points on the inner boundary and $U_0 = 0$ to all points on the outer boundary. An initial value is assigned to all interior mesh points:

$$U^0_{J,K} = (Y - J)/(Y - LL1) \qquad LL1 + 1 \leq J \leq Y - 1, \quad 1 \leq K \leq LR2 \,, \tag{29}$$

$$U^0_{J,K} = (J - 1)/(UL1 - 1) \qquad 2 \leq J \leq UL1 - 1, \quad 1 \leq K \leq UR2 \,, \tag{30}$$

$$U^0_{J,K} = U(J,LR2)[(Z - K)/(Z - LR2)] \qquad 2 \leq J \leq Y - 1, \quad UR2 + 1 \leq K \leq Z - 1 \,. \tag{31}$$

3.2.2 Relaxation Process

The relaxation procedure consists of scanning successive columns from left to right and continuously modifying the potential according to Eq. (24):

$$U^{n+1}_{j,k} = \frac{1}{4}\left(U^{n+1}_{j-1,k} + U^{n}_{j+1,k} + U^{n+1}_{j,k-1} + U^{n}_{j,k+1}\right) . \tag{32}$$

Equation (24) is modified along the mirror surface (Column 1):

$$U^{n+1}_{j,1} = \frac{1}{4}\,[2U(j,2) + U(j - 1,1) + U(j + 1,1)] \,. \tag{33}$$

3.2.3 Capacitance Calculation

The capacitance calculation consists of determining an integration contour around the inner conductor, calculating the total charge according to Eq. (27), and dividing by the potential difference. Line segments L2 and L3 lie halfway between the inner conductor and the ground plane. Line segments L1 and L3 are the same distance from the inner conductor. That is, let

$$IUL1 = UL1 - [(LL1 + Y)/2 - LL1] \ , \tag{34}$$

$$ILL1 = (LL1 + Y)/2 \ , \tag{35}$$

$$LUR2 - (LR2 - Z)/2 \ . \tag{36}$$

Thus the points (IUL1,1), (IUL1, IUR2), (ILL1, IUR2) and (ILL1,1) determine the three relevant line segments (Fig. 5) and the total charge may be calculated according to the methods of Sec. 3.1.

3.3 Experiment

Impedance predictions from the finite difference analysis are compared with experimental results from a fabricated stripline. The impedance of the stripline is determined by means of time domain reflectometry (TDR).[9] TDR analysis is based on the reflection of voltage from a discontinuity or perturbation in a transmission system. The components of the HP 7S12 TDR system include a fast-rising voltage step generator ($t_r < 25$ ps), a sampling oscilloscope ($t_r < 30$ ps), and a transmission line system. The reflection coefficient vs signal propagation time is read directly from the oscilloscope, and the impedance of the stripline may be calculated from Eq. (12).

A comparison between the finite difference predictions obtained using the computer program in Appendix 1 and experimental results is shown in Fig. 6 for a stripline structure. Agreement of better than 1% between theory and experiment is noted for all four cases. Exact mesh size details are given in Appendix 2.

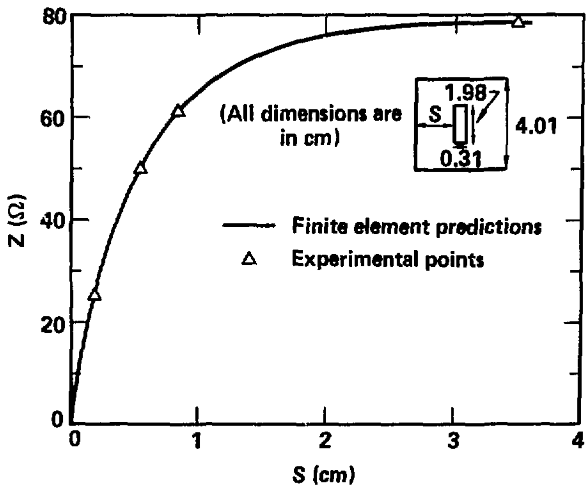

Figure 6. Finite element impedance predictions and experimental results.

4. Variable Impedance Stripline to Pulse Excitation

We are interested in determining the reflected voltage from a variable impedance stripline system (Fig. 7). Note that the impedance variations for the structure of interest are the result of differences in conductor to ground plane spacing in the direction of pulse propagation. We assume the following:

1. A pure TEM mode is excited at $Z = 0$ (and extracted after reflection).
2. Coupling to higher order modes along the direction of propagation is negligible.
3. The stripline system is non-dispersive.

4.1 Theory

A schematic representation of the variable impedance stripline is shown in Fig. 8. We have approximated the continuous impedance variation by a series of steps in the transmission line. Reflection and transmission from a single discontinuity have been examined in Sec. 2. Here, we analyze reflection and transmission from several discontinuities.

Consider two time-separated discontinuities (Fig. 9); the actual reflection caused by ρ_2 will be altered by ρ_1 before the actual ρ_2 arrives at the TDR.[9] Manipulating Eqs. (9), (12), and (13) we obtain

$$V_+(1 + \rho) = \tau \; . \tag{37}$$

The incident and reflected voltages from the second discontinuity are $V_+(1 + \rho_1)$ and $V_+(1 + \rho_1)\rho_2$, respectively. The voltage appearing at the oscilloscope is $V_+(1 + \rho_1)(1 - \rho_1)$. Note that the reflection coefficient changes sign for travel in the opposite direction. Then,

$$\frac{\rho_2'}{\rho_2} = \frac{\text{measured value}}{\text{true value}} = (1 + \rho_1)(1 - \rho_1) = 1 - \rho_1^2 \; . \tag{38}$$

For a system of three discontinuities

$$\frac{\rho_3'}{\rho_3} = \frac{\text{measured value}}{\text{true value}} = (1 - \rho_1^2)(1 - \rho_2^2) \; . \tag{39}$$

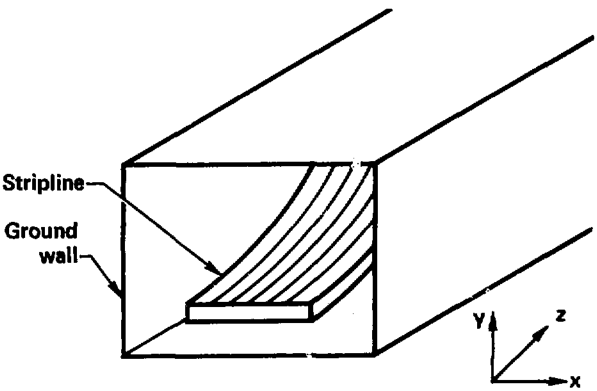

Figure 7. Variable impedance stripline.

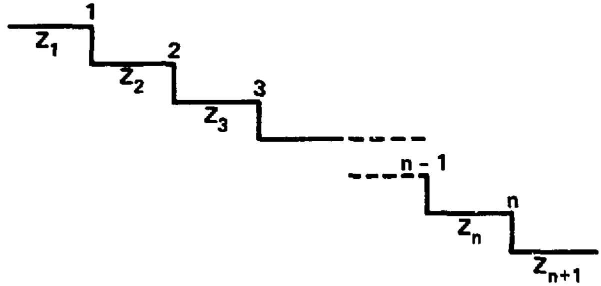

Figure 8. Schematic representation of variable impedance stripline.

By induction, the error in the nth discontinuity with $n-1$ discontinuities between it and the sampling scope is

$$\frac{\rho_n'}{\rho_n} = (1 - \rho_1^2)(1 - \rho_2^2) \cdots (1 - \rho_{n-1}^2) \; . \tag{40}$$

The relevant computer program is described in Appendix 3. The reflection coefficient at each point along the direction of pulse propagation is calculated from the quasi-static impedance. The velocity of propagation is

$$v = \frac{1}{\sqrt{LC}} = c \; . \tag{41}$$

From Eqs. (40) and (41), the reflection coefficient vs pulse propagation time is calculated, and the short pulse behavior of a variable impedance stripline is thus determined.

4.2 Experiment

Experimental results from a variable impedance stripline structure are subsequently compared with predictions. Again, the short-pulse behavior is determined by time domain reflectometry. A structure similar to that of Fig. 7 is fabricated. Actual dimensions along with finite element impedance predictions are given in Fig. 10. The structure is approximately 30 cm long (z direction), and the impedance variations along the z direction can be arbitrarily adjusted by varying the conductor-to-ground-plane spacing with a series of micrometers.

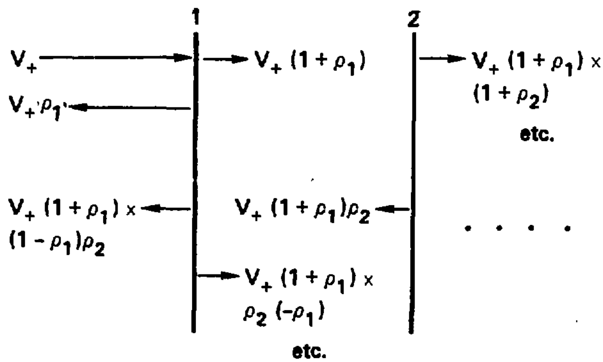

Figure 9. Reflection and transmission from two time separated discontinuities.

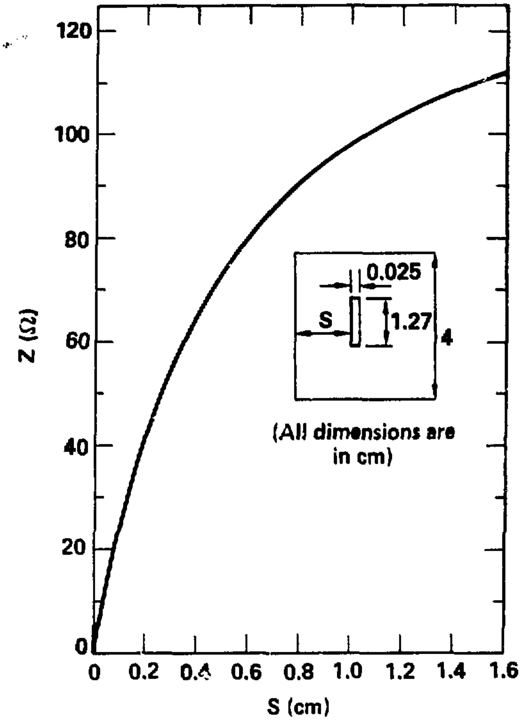

Figure 10. Finite element impedance predictions used for transient analysis.

The computer predictions and experimental results of Figs. 11 to 13 are obtained as follows:

1. Measure the conductor-to-ground-plane spacing, which varied along the z direction.
2. Calculate the corresponding impedance using the finite difference formulation of Sec. 3.
3. Determine the reflection coefficient vs signal propagation time using the analysis of Sec. 4.
4. Compare to results obtained from an HP 7S12 TDR.

Good agreement between theory and experiment is noted for all three cases, although the computer predictions tend to overestimate the reflection coefficient at later times. We attribute this discrepancy to rapid changes in the conductor-to-ground plane spacing along the z direction that cause unwanted coupling to higher order modes and subsequent invalidation of the assumptions of Sec. 4.

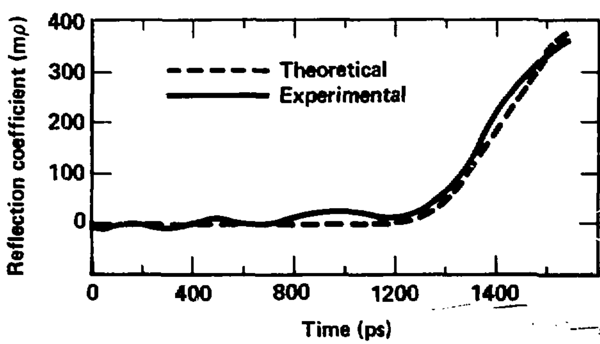

Figure 11. Transient predictions and experimental results.

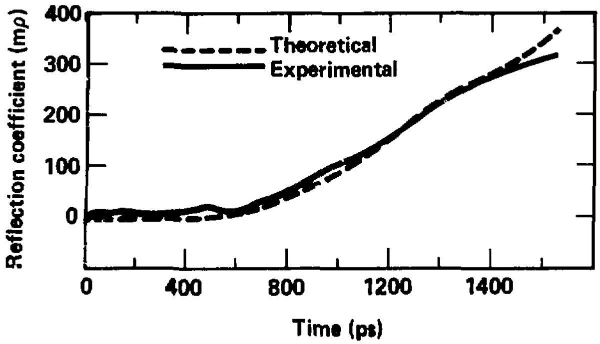

Figure 12. Transient predictions and experimental results.

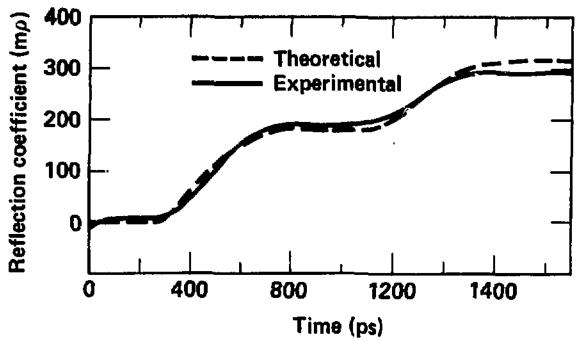

Figure 13. Transient predictions and experimental results.

5. Conclusion

We describe a simple method to predict the transient response of variable impedance stripline to pulse excitation. This technique uses a finite difference based quasi-static impedance formulation to calculate the reflection coefficient at each point along the direction of pulse propagation; the short pulse behavior of the structure is thus determined. Excellent correlation between the finite difference impedance predictions and experimental results is noted. Incorporation of the finite difference impedance calculations into the transient analysis yields good agreement between predictions and results obtained by time domain reflectometry (TDR).

References

1. *1983 Laser Program Annual Report*, Lawrence Livermore National Laboratory, Livermore, CA, UCRL-50021-83 (1984), pp. 2-20 to 2-21.
2. S. Ramo, J. Whinnery, and T. Van Duzer, *Fields and Waves in Communication Electronics* (John Wiley and Sons, New York, 1965), pp. 23–61.
3. R. A. Waldon, *Theory of Guided Electromagnetic Waves* (Van Nostrand Reinhold, London, 1969), pp. 157–170.
4. M. V. Schneider, "Computation of Impedance and Attenuation of TEM-Lines by Finite Difference Methods," *IEEE Trans. Microwave Theory and Techniques* **13**, 793–800 (1965).
5. K. J. Binns and P. J. Lawrenson, *Analysis and Computation of Electric and Magnetic Field Problems* (Pergamon Press, Oxford, 1973), pp. 241–285.
6. L. F. Richardson, "The Approximate Arithmetical Solution by Finite Differences of Physical Problems Involving Differential Equations, with an Application to the Stresses in a Masonry Dam," *Phil. Trans.* **210A**, 307 (1911).
7. P. Silvester and M. S. Hseih, "Finite Element Solution of 2-Dimensional Exterior Field Problems," *Proc. IEE* **118**, 1743 (1971).
8. Harry E. Green, "The Numerical Solution of Some Important Transmission-Line Problems," *IEEE Trans. Microwave Theory and Techniques* **13**, 676–692 (1965).
9. P. E. Allen, *Analysis of Transmission Systems by Time Domain Reflectometry*, Lawrence Livermore National Laboratory, Livermore, CA, UCRL-12319 (1965).

SP/js

Appendix 1

```
C     FINITE DIFFERENCE PROGRAM (MICROSOFT FORTRAN) TO CALCULATE
C     IMPEDANCE OF STRIPLINE SURROUNDED ON ALL SIDES BY GROUND
C     PLANES.  WRITTEN BY GLEN MCWRIGHT, AUGUST 1984.
      INTEGER UL1(10),UL2(10),UR1(10),UR2(10),LL1(10),LL2(10)
      INTEGER LR1(10),LR2(10),Y(10),Z(10),J,K,N(10),A,M
      INTEGER IUL1,ILL1,IUR2,B,Q,NQ,YQ,UR1Q,ZQ,UR2Q,LL1Q
      REAL U(500,101),AVG1,S1,S2,S3,IMP
C     INPUT NUMBER OF CASES (MAX OF 999)
      READ (*,3) B
    3 FORMAT (I3)
      DO 8 M=1,B
C     INPUT COORDINATES OF CENTER CONDUCTOR, GROUND PLANES, AND
C     NUMBER OF ITERATIONS
      READ (*,5) UL1(M),UL2(M),UR1(M),UR2(M),LL1(M),LL2(M),
     *LR1(M),LR2(M),Y(M),Z(M),N(M)
    5 FORMAT (10I3,I4)
    8 CONTINUE
C     SET POTENTIAL TO ZERO THROUGHOUT STRUCTURE
      DO 400 Q=1,B
      DO 20 J=1,Y(Q)
      DO 10 K=1,Z(Q)
      U(J,K)=0.
   10 CONTINUE
   20 CONTINUE
C     SET POTENTIAL TO UNITY ON CENTER CONDUCTOR
      DO 40 J=UL1(Q),LL1(Q)
      DO 30 K= UL2(Q),UR2(Q)
      U(J,K)=1.
   30 CONTINUE
   40 CONTINUE
C     CALCULATE INITIAL GUESSES FOR POTENTIAL THROUGHOUT STRUCTURE
      DO 60 J=LL1(Q)+1,Y(Q)-1
      DO 50 K=1,LR2(Q)
      U(J,K)= 1.*(Y(Q)-J)/(Y(Q)-LL1(Q))
   50 CONTINUE
   60 CONTINUE
      DO 80 J=2,UL1(Q)-1
      DO 70 K=1,UR2(Q)
      U(J,K)=1.*(J-1)/(UL1(Q)-1)
   70 CONTINUE
   80 CONTINUE
      DO 100 J=2,Y(Q)-1
      DO 90 K=UR2(Q)+1,Z(Q)-1
      AVG1= 1.*(Z(Q)-K)/(Z(Q)-LR2(Q))
      U(J,K)= AVG1*U(J,LR2(Q))
   90 CONTINUE
  100 CONTINUE
      NQ=N(Q)
      YQ=Y(Q)
      UR1Q=UR1(Q)
      UR2Q=UR2(Q)
      ZQ=Z(Q)
      LL1Q=LL1(Q)
```

```
C       BEGIN RELAXATION LOOP
        DO 140 A=1,NQ
        DO 110 J=2,UR1Q-1
        U(J,1)= 0.25*(2.*U(J,2)+U(J-1,1)+U(J+1,1))
  110   CONTINUE
        DO 115 J=LL1Q+1,YQ-1
        U(J,1)= 0.25*(2.*U(J,2)+U(J-1,1)+U(J+1,1))
  115   CONTINUE
        DO 120 K=2,UR2Q
        DO 117 J=2,UR1Q-1
        U(J,K)=0.25*(U(J-1,K)+U(J+1,K)+U(J,K-1)+U(J,K+1))
  117   CONTINUE
        DO 119 J=LL1Q+1,YQ-1
        U(J,K)= 0.25*(U(J-1,K)+U(J+1,K)+U(J,K-1)+U(J,K+1))
  119   CONTINUE
  120   CONTINUE
        DO 135 K= UR2Q+1,ZQ-1
        DO 130 J=2,YQ-1
        U(J,K)= 0.25*(U(J-1,K)+U(J+1,K)+U(J,K-1)+U(J,K+1))
  130   CONTINUE
  135   CONTINUE
  140   CONTINUE
        WRITE (*,150) UL1(Q),UL2(Q),UR1(Q),UR2(Q),LL1(Q),LL2(Q),
       *LR1(Q),LR2(Q),Y(Q),Z(Q),N(Q)
  150   FORMAT (1X,11I3)
C       DETERMINE GAUSSIAN SURFACE OF INTEGRATION
        IUL1= UL1(Q)-((LL1(Q)+Y(Q))/2-LL1(Q))
        ILL1= (LL1(Q)+Y(Q))/2
        IUR2= (LR2(Q)+Z(Q))/2
C       CALCULATE CHARGE ALONG EACH SEGMENT OF GAUSSIAN SURFACE
        S1=0.
        DO 250 K=2,IUR2-1
        S1= S1+0.5*(U(ILL1-1,K)-U(ILL1+1,K))
  250   CONTINUE
        S1= 0.25*(U(ILL1-1,IUR2)-U(ILL1+1,IUR2))+S1
        S2=0.
        DO 270 J=IUL1+1,ILL1-1
        S2= S2+0.5*(U(J,IUR2-1)-U(J,IUR2+1))
  270   CONTINUE
        S2=0.25*(U(ILL1,IUR2-1)-U(ILL1,IUR2+1))+
       *0.25*(U(IUL1,IUR2-1)-U(IUL1,IUR2+1))+S2
        S3=0.
        DO 290 K=2,IUR2-1
        S3=S3+0.5*(U(IUL1+1,K)-U(IUL1-1,K))
  290   CONTINUE
        S3=0.25*(U(IUL1+1,IUR2)-U(IUL1-1,IUR2))+S3
C       CALCULATE TOTAL CHARGE
        CH= 2.*(S1+S2+S3)+0.5*(U(IUL1+1,1)-U(IUL1-1,1))+
       *0.5*(U(ILL1-1,1)-U(ILL1+1,1))
        IMP=377./CH
        WRITE (*,300) IMP
  300   FORMAT (1X,F8.5)
  400   CONTINUE
        STOP
        END
```

Appendix 2

Computer input for finite element calculations of Fig. 6. mesh size, h = 0.1 cm.

S = 0.3 cm	0950010950110980010980111101021999
S = 0.4	0940010940110970010970111101021999
S = 0.5	0930010930110960010960111101021999
S = 0.6	0920010920110950010950111101021999
S = 0.7	0910010910110940010940111101021999
S = 0.8	0900010900110930010930111101021999
S = 0.9	0890010890110920010920111101021999
S = 1.0	0880010880110910010910111101021999
S = 1.4	0840010840110870010870111101021999
S = 1.8	0800010800110830010830111101021999
S = 2.4	0740010740110770010770111101021999
S = 3.0	0680010680110710010710111101021999
S = 3.6	1620011620111650011650111201021999

Appendix 3

```
C       PROGRAM (MICROSOFT FORTRAN) TO CALCULATE TRANSIENT
C       RESPONSE OF STRIPLINE TO PULSE EXCITATION. WRITTEN
C       BY GLEN MCWRIGHT, NOVEMBER 1984.
        INTEGER A,B,C,D,E,F,G
        REAL Z(50),P(50),PR(50),TDR(50),PP(50)
C       INPUT NUMBER OF IMPEDANCE STEPS
        READ (*,5) A
      5 FORMAT (I3)
        DO 10 B=1,A
C       INPUT IMPEDANCE
        READ (*,8) Z(B)
      8 FORMAT (F7.2)
     10 CONTINUE
        DO 20 C=1,A-1
C       CALCULATE REFLECTION COEFFICIENT
        P(C)= (Z(C+1)-Z(C))/(Z(C)+Z(C+1))
     20 CONTINUE
C       CALCULATE REDUCED REFLECTION COEFFICIENT
        PR(2)= (1.-(P(1)*P(1)))
        DO 30 D=3,A-1
        PR(D)= (1.-(P(D-1)*P(D-1)))*PR(D-1)
     30 CONTINUE
        PP(1)=P(1)
        DO 40 G=2,A-1
        PP(G)=PR(G)*P(G)
     40 CONTINUE
        TDR(1)=PP(1)
        DO 50 E=2,A-1
        TDR(E)=TDR(E-1) +PP(E)
     50 CONTINUE
C       PRINT REDUCED REFLECTION COEFFICIENT AT EACH IMPEDANCE STEP
        DO 60 F=1,A-1
        WRITE (*,55) TDR(F)
     55 FORMAT (1X,F8.5)
     60 CONTINUE
        STOP
        END
```